Prediction of radiation pneumonitis after definitive radiotherapy for locally advanced non-small cell lung cancer using multi-region radiomics analysis

Daisuke Kawahara (daika99@hiroshima-u.ac.jp)
Department of Radiation Oncology, Graduate School of Biomedical Health Sciences, Hiroshima University, Hiroshima, 734-8551, Japan

Nobuki Imano
Department of Radiation Oncology, Graduate School of Biomedical Health Sciences, Hiroshima University, Hiroshima, 734-8551, Japan

Riku Nishioka
Medical and Dental Sciences Course, Graduate School of Biomedical & Health Sciences, Hiroshima University, Hiroshima, 734-8551, Japan

Kouta Ogawa
School of Medicine, Hiroshima University, Hiroshima, 734-8551, Japan

Tomoki Kimura
Department of Radiation Oncology, Graduate School of Biomedical Health Sciences, Hiroshima University, Hiroshima, 734-8551, Japan

Taku Nakashima
Department Molecular and Internal Medicine, Graduate School of Biomedical Health Sciences, Hiroshima University, Hiroshima, 734-8551, Japan

Hiroshi Iawamoto
Department Molecular and Internal Medicine, Graduate School of Biomedical Health Sciences, Hiroshima University, Hiroshima, 734-8551, Japan

Kazunori Fujitaka
Department Molecular and Internal Medicine, Graduate School of Biomedical Health Sciences, Hiroshima University, Hiroshima, 734-8551, Japan

Noboru Hattori
Department Molecular and Internal Medicine, Graduate School of Biomedical Health Sciences, Hiroshima University, Hiroshima, 734-8551, Japan

Yasushi Nagata
Department of Radiation Oncology, Graduate School of Biomedical Health Sciences, Hiroshima University, Hiroshima, 734-8551, Japan

Research Article

Keywords: Radiomics, Machine learning, Radiation pneumonitis

Posted Date: April 26th, 2021

DOI: https://doi.org/10.21203/rs.3.rs-428285/v1

Version of Record: A version of this preprint was published at Scientific Reports on August 10th, 2021. See the published version at https://doi.org/10.1038/s41598-021-95643-x.

Abstract

Objective To predict grade 2 radiation pneumonitis (RP) in locally advanced non-small cell lung cancer (NSCLC) patients with high accuracy by using multi-region radiomics analysis.

Material and Methods Data from 77 patients with NSCLC who underwent definitive radiotherapy from 2008 to 2018 were analyzed. Radiomic feature extraction from the whole lung (whole-lung radiomics analysis) and imaging- and dosimetric-based segmentation (multi-region radiomics analysis) were performed. The data were split into 2 sets: 54 tumors for model training and 23 tumors for model testing. Patients with RP grade ≥2 or RP grade <2 was classified. Models were built with least absolute shrinkage and selection operator logistic regression and applied to the set of candidate predictors. To build predictive models with clinical features, machine-learning methods with neural network classifiers were used. The precision, accuracy, and sensitivity by generating confusion matrices and the areas under the receiver operating characteristic curve (AUC) for each model were evaluated.

Results A total of 49383 radiomics features per patient image were extracted from the radiotherapy planning computed tomography scan. We identified 4 features selected in the whole-lung radiomics analysis and 13 radiomics features selected in the multi-region radiomics analysis for the classification. Out of 13 features, the median and high-dose region were selected from the shape analysis. The features of local intensity roughness and variation were selected from the statistical and texture analysis. The accuracy, specificity, sensitivity, and AUC were 80.1%, 79.2%, 88.9%, and 0.84 for our new method of multi-region radiomics analysis, respectively, which was improved from 60.8%, 64.6%, 53.8%, and 0.62 for whole-lung radiomics analysis.

Conclusions The developed multi-region radiomics analysis can help predict grade 2 RP for NSCLC after definitive radiotherapy. The radiomics features in the median- and high-dose regions, and that of local intensity roughness and variation were important factors in predicting grade 2 RP.

1. Introduction

Chemoradiotherapy (CRT) is the standard treatment for unresectable locally advanced non-small cell lung cancer (NSCLC). However, CRT for NSCLC carries the risk of developing radiation pneumonitis (RP) [1]. Although the development of immunotherapy has been shown to significantly improve survival after CRT [2], immunotherapy cannot be continued when RP develops. Previous studies have developed many indicators for predicting grade 3 RP as a serious adverse event [3—7]. However, it is extremely important to predict grade 2 RP because immunotherapy cannot be continued if grade 2 or higher RP occurs.

Various indicators have been shown so far for predicting grade 2 and 3 RP by CRT for NSCLC, including sex, smoking status, tumor location, age, and pulmonary comorbidity [8, 9]. These patient backgrounds should be carefully considered to predict RP. Another approach to predict RP is dosimetric predictors. The mean lung dose or the volume of the lung receiving > 20 Gy (V20), have been reported as the best correlated predictors of RP [10, 11]. We previously reported the importance of reducing high dose area by

analyzing NSCLC patients who received 3D-CRT or intensity-modulated RT (IMRT) [12] These DVH parameters have been considered individually, however these factors need to be considered comprehensively. Besides, there are individual differences in the risk of developing RP among patients with the same dosimetric predictors probably because of patients' background. Therefore, predictive indicators that consider both individual patient background factors and all kinds of dosimetric factors are needed.

Recently, radiomics has been proposed to explore the correlation between medical images and underlying genetic information and other characteristics [13]. It has been used for classifying patients and evaluating their risk in order to tailor and customize prescribed oncological treatments. Texture features from computed tomography (CT) images show utility for differentiating lung phenotypes resulting from patients' lung background [14]. Krafft et al. proposed a predictive model for RP toxicity after radiotherapy using pretreatment CT-based radiomics features extracted from whole-lung volume [15]. They proposed a predictive model with CT-based radiomics features extracted from only the whole-lung region, which reflect patients' lung background but not dosimetric factors. We hypothesized that radiomics analysis can be improved by increasing a region of interest (ROI) which reflect all kinds of dosimetric factors. The past studies reported the usability of the increasing the radiomics features by adding the ROI in the outer region of the tumor for accuracy improvement of the prediction [16, 17]. These approaches showed that the imaging features from multi-region radiomics analysis were useful for predicting treatment outcome; however, these ROI did not reflect dosimetric factors, and no report has utilized this method to predict RP.

In the current study, we proposed a method of multi-region radiomics analysis that can reflect both patients' lung background and all kinds of imaging and dosimetric factors in the imaging and dosimetric-based segmentations to predict grade 2 RP in locally advanced NSCLC.

2. Materials And Methods

2.1 Patients

The eligibility criteria for this study were as follows: histologically confirmed NSCLC; clinical stage II, IIIA, IIIB, or IVA according to the 8th TNM staging system of the International Union Against Cancer (UICC); no distant organ metastasis diagnosed by CT, magnetic resonance imaging (MRI), or positron emission tomography CT (PET-CT); had been irradiated using three-dimensional conformal radiotherapy (3D-CRT); and had been followed until the onset of RP of grade 2 or higher, or for more than 6 months after the completion of treatment. Hiroshima University review board approved this retrospective study (E-1656). The ethics committee approved that this retrospective study can waive informed consent. The methods were performed by the relevant guidelines and regulations.

2.2 Image Acquisition

Figure 1 shows the workflow of the current study. CT imaging of a patient was performed during free breathing on a CT scanner (Lightspeed RT16, GE Healthcare; Little Chalfont, UK). The slice thickness and slice interval were 2.5 mm.

2.3 Radiotherapy treatment

Radiotherapy was performed with three-dimensional radiotherapy treatment planning for all patients. Gross tumor volume (GTV) included the primary tumor and lymph node (LN) metastasis. The clinical target volume (CTV) for the primary lesion and LNs was defined as the GTV with a 3–5 mm and 0–3 mm margin in all directions, respectively. Margins of 5–10 mm were added to the CTV to determine the planning target volume (PTV). Elective nodal irradiation was omitted in all patients. A total irradiation dose of 60–74 Gy was administered for PTV. Dose calculation algorithm was used a collapsed cone convolution superposition/convolution algorithm (CCCS), which is available in Pinnacle3 (Philips Radiation Oncology Systems, Fitchburg, WI)

2.4 Follow-up

Patients were followed up every month after treatment completion until 6 months, and every 3 months thereafter. Patients received a chest X-ray every month and chest-to-pelvis CT at 1-, 3-, and 6-month follow-up visits and every 3–6 months thereafter. RP was evaluated using the Common Terminology Criteria for Adverse Events (CTCAE) version 5.0 [18]. More specifically, we defined grade 2 RP as when any drug was used for RP symptoms.

2.5 Radiomics Analysis

First, normalization (z-score transformation) of image intensity was performed on the whole image to transform arbitrary CT values into standardized intensity ranges, thereby avoiding heterogeneity bias. Then, the entire CT imaging dataset was analyzed to extract textural features from the segmentations for the radiotherapy plans and dose distribution.

The current study proposed two radiomics analyses: one is the whole-lung radiomics analysis proposed by Kraft et al. in which radiomics features are extracted only in the whole-lung region [15], and the other is multi-region radiomics analysis in which radiomics features are extracted in the imaging-based segmentation and dosimetric-based segmentation. CT image segmentation was defined as imaging-based segmentation, as shown in Table 1(a). In addition to the GTV, CTV, and PTV radiomics features that were used in treatment planning, the shell radiomics features of the region around the GTV, CTV, and PTV, and inner radiomics features of the region that excluded the tumor boundaries were extracted.

RP occurs outside the tumor, and lungs that receive low doses (5 Gy or 20 Gy) are associated with RP [19, 20]. Thus, the radiomics features of lungs overlapping with the outside of the GTV and PTV were analyzed. Moreover, the target received a higher dose, and normal-lungs or whole lungs that received lower to higher doses were added to the analysis as dosimetric-based segmentation, as shown in Table 1(b).

Feature extraction was performed using Pyradiomics, an open-source package in Python [21]. A detailed list of the radiomics features is shown in Table S1 and Table S2.

Table 1
(a). Imaging-based segmentation list in multi-region radiomics analysis

Imaging-based segmentation list			
GTV	GTV-2mm	GTV + 5mm	GTV + 10mm
	(GTV + 5mm)-GTV	(GTV + 10mm)-GTV	
CTV	CTV-GTV		
PTV	PTV + 5mm	PTV + 10mm	PTV + 20mm
	PTV-GTV		
	(PTV + 5mm)-PTV	(PTV + 10mm)-PTV	(PTV + 20mm)-(PTV + 5mm)
Lung	Lung-GTV	Lung-PTV	
	Lung-(GTV + 5mm)		
	Lung-(PTV + 5mm)	Lung-(PTV + 10mm)	Lung-(PTV + 20mm)
GTV, gross tumor volume; CTV, clinical target volume; PTV, planning target volume.			

Table 1
(b). Dosimetric-based segmentation list in multi-region radiomics analysis

Dosimetric-based segmentation list
Lung received 5–60 Gy: Lung∩5—60 Gy
(Lung-GTV) received 5–60 Gy: Lung-GTV∩5—60 Gy
Lung-PTV received 5–60 Gy: Lung-PTV∩5—60 Gy
PTV received 40–60 Gy: PTV∩40—60 Gy
(PTV + 5mm) received 30–60 Gy: PTV + 5mm∩30—60 Gy
(PTV + 10mm) received: PTV + 10mm∩20—60 Gy
(PTV + 20mm) received 10–60 Gy: PTV + 20mm∩10—60 Gy
GTV, gross tumor volume; CTV, clinical target volume; PTV, planning target volume.

A list of 50 quantitative features including 21 first-order features, 13 shape features, and 93 texture analysis features (such as gray-level size zone matrix [GLSZM] features and gray-level run length matrix [GLRLM] features) were extracted. Moreover, the CT images leave the image unchanged as the original, and these are preprocessed with a wavelet imaging filter. The wavelet filter has low-pass (L) and high-

pass (H) filters. The decompositions are constructed in the x-, y-, and z-directions. For example, HLL is then interpreted as the high-pass sub-band, resulting from directional filtering of X with a high-pass filter in the x-direction, a low-pass filter in the y-direction, and a low-pass filter in the z-direction. In the current study, 8 wavelet decompositions (HLL, LHL, LHH, LLH, HLH, HHH, HHL, and LLL) were performed. Each feature was computed separately with each of the aforementioned preprocessing steps. A total of 837 features were analyzed for each segmentation in this study.

2.6 Prediction model

The interaction between radiomics features were evaluated with VIF analysis. We used variance inflation factor (VIF), removing factors of VIF > 10. Next, the least absolute shrinkage and selection operator (LASSO) regression model, which is suitable for the regression of high-dimensional data for whole-lung radiomics analysis and multi-region radiomics analysis, was used with MATLAB code (MathWorks; Natick, MA) [22, 23]. LASSO performs feature selection during model construction by penalizing the respective regression coefficients. As this penalty is increased, more regression coefficients shrink to zero, resulting in a more regularized model. The most significant predictive features were selected from among all candidate features in the training set.

The objective of this study was to stratify patients into two labeled classes using different machine-learning (ML) classifiers. In this regard, patients with RP grade ≥ 2 were labeled as 1, and patients with RP grade < 2 were labeled as 0. This was also repeated to classify patients according to stage. ML-based classification was performed using the neural-network method. Here, all patients were randomly partitioned into either a training set (55% patients), validation set (15% patients), or testing set (30% patients). The ratio of labels of RP was the same for the training and test dataset. To find the best predictive models for these classifications, we tested different combinations of feature selection and classification methods. Classifiers were trained using the ten-fold cross-validation method, and their predictive performance was then evaluated using the area under the receiver operator characteristic (ROC) curve (AUC). As shown in Fig. S1, the training-validation-testing processes were repeated 5 times for the 5-fold cross-validation. The predictive performance of all models was compared based on the mean AUC.

3. Results

A total of 77 patients were included in this study. The characteristics of the patients and their tumors are presented in Table S3. In total, 32 of 77 patients (42%) developed grade 2 or higher RP.

From the radiomics analysis, a total of 49383 features were extracted from CT images. By the VIF-based feature reduction, the number of radiomics features were reduced from 49383 to 32541. In the whole-lung radiomics analysis, 4 features were selected using the LASSO regression model, as shown in Table 2(a) and Fig. S2. These features included the minimum and median CT number and the magnitude of the fineness and coarseness of the texture. All radiomics features used a wavelet filter. Features with non-

uniformity, local intensity roughness, and a higher ratio of the region with high pixel numbers were selected.

In the multi-region radiomics method, 13 features were selected using the LASSO regression model, as shown in Table 2(b) and Fig. S3. Out of 13 features, 5 features were selected from the shape analysis of the dosimetric segmentation, 3 features were selected from statistical analysis, and 5 features were selected from texture analysis. From the shape analysis, the 5 shape features of in the median dose of 20—30 Gy and high-dose of 60 Gy regions from the overlapping region of dosimetric segmentation and lung were selected. As for the statistical and texture analysis, 4 features were selected from the whole lung and normal-lung regions, 2 features were selected from the dosimetric segmentation, and 2 features were selected from the overlapping region of dosimetric segmentation and lung.

Figure 2(a) shows the validation of the performance of the predictive model according to ROC metrics with 5-fold cross validation in the whole-lung radiomics analysis. Table 3(a) shows the results of the accuracy, sensitivity, specificity, and AUC of the prediction model in the whole-lung radiomics analysis for the training and testing data. The average accuracy of the 5 models was 65.2% with the training data. The average accuracy, sensitivity, and specificity of the test data were 60.8%, 64.6%, and 53.8%, respectively. The AUC was 0.55 for the first model, 0.65 for the second model, 0.58 for the third model, 0.71 for the fourth model, and 0.63 for the fifth model. The average AUC with 5-fold cross validation was 0.63 ± 0.05.

Next, we applied multi-region radiomics analysis to improve the accuracy of prediction for RP. Figure 2(b) shows the performance of the predictive model was validated according to the ROC metrics with 5-fold cross validation in the multi-region radiomics analysis. Table 3(b) shows the results of the accuracy, sensitivity, specificity, and AUC of the prediction model in the whole-lung radiomics analysis and the multi-region radiomics analysis for the training and testing data. The average accuracy of the 5 models was 82.3% with the training data. The average accuracy, sensitivity, and specificity of the test data were 80.1%, 79.2%, and 88.9%, respectively. The average accuracy, sensitivity, specificity, and AUC in the multi-region radiomics analysis were improved from those in the whole-lung radiomics analysis.

Table 2
(a). Selected features by LASSO Cox-regression in the whole-lung-region radiomics analysis

ROI	Imaging filter	Feature	
Lung	wavelet-LLH	firstorder	Minimum
Lung	wavelet-HHL	firstorder	Median
Lung	wavelet-HHH	glcm	Correlation
Lung	wavelet-HHL	glcm	Correlation

Table 2
(b). Selected features by LASSO Cox-regression in the multi-region radiomics analysis

ROI	Imaging filter	Feature	
Lung-GTV	wavelet-LLH	glcm	JointAverage
Lung-GTV	wavelet-LLH	firstorder	Minimum
Lung-GTV	wavelet-HHL	gldm	Small Dependence Low Gray Level Emphasis
Lung-PTVad20	wavelet-LLH	ngtdm	Strength
5.00 Gy	wavelet-LHL	firstorder	Skewness
20.00 Gy	wavelet-LHL	firstorder	Skewness
30Gy∩Lung-GTV	wavelet-HLL	gldm	Gray Level Non-Uniformity
50Gy∩Lung-GTV	wavelet-LHL	glszm	Large Area High Gray Level Emphasis
60Gy∩Lung-GTV	original	shape	MajorAxis
60Gy∩Lung-GTV	original	shape	Flatness
20Gy∩Lung	original	shape	MinorAxis
30Gy∩Lung	original	shape	MajorAxis
60Gy∩Lung-PTV	original	shape	Maximum 3D Diameter

Table 3
(a). Assessment of the predictive performance of the predictive model for training and testing data in the whole-lung radiomics analysis.

	Training (%)	Test (%)
Sensitivity	65.2(59–72.7)	64.6(57.1–70.6)
Specificity	64.8(53.3–83.3)	53.8(33.3–70.6)
Accuracy	64.7(61.9–71.4)	60.8(56.5–65.2)
AUC	-	0.62(0.55–0.71)
AUC, area under the curve.		

Table 3
(b). Assessment of the predictive performance of the predictive model for training and testing data in multi-region radiomics analysis.

	Training (%)	Test (%)
Sensitivity	79.7(69.7–86.7)	79.2(71.4–92.9)
Specificity	77.6(66.7–84.6)	88.9(55.6–100)
Accuracy	82.3(73.9–87.0)	80.1(65.2–91.3)
AUC	-	0.84(0.73–0.92)

AUC, area under the curve.

4. Discussion

RP is a very important adverse event in radiotherapy for NSCLC, and if it can be predicted, it will be useful information for deciding the treatment policy, such as prescription dose and follow-up interval.

In the past, grade 3 RP was applied to predict RP. Dang et al. reported that grade 2 and grade 3 RP have different predictors [24]. Therefore, predictors of grade 2 RP require an original approach. Since immunotherapy has revolutionized the treatment of lung cancer [25], it is very important to predict grade 2 RP because it prevents the continuation of immunotherapy. In the current study, we focused on finding a new method to predict grade 2 RP. A previous report showed that background factors such as sex, smoking status, tumor location, age, and pulmonary comorbidity have been identified as potential risks [8, 9]. Dosimetric factors, such as the mean lung dose or V20, and other several DVH parameters have also been reported as the best correlated predictors of RP. It is necessary to develop predictors that take both these factors into consideration.

Currently, radiomics approaches have been used to improve diagnostic quality or to predict treatment outcomes by using medical images that have only been used for radiation diagnosis, treatment planning, and follow-up after treatment. Krafft et al. combined radiomics features extracted from whole-lung images with clinical and dosimetric features and significantly improved the RP model for grade 3 RP [15]. The cross-validated AUC of their model was 0.68. The current study compared the prediction model using the whole-lung radiomics analysis that was performed by Krafft et al. and multi-region radiomics analysis, which was proposed as a new method in the current study. We were able to reproduce the same degree of accuracy by using a method like that of Krafft et al., as though we predicted grade 2 RP rather than grade 3. Furthermore, we could improve the quality by using multi-region radiomics, which had superior accuracy, sensitivity, specificity, and AUC compared to whole-lung radiomics analysis.

In the multi-region radiomics analysis, the radiomics features of local intensity roughness and variation were selected from the CT image. Previous study showed that the increasing in radiologic density within the irradiated lung was to be a predictor for the RP. Thus, the radiation pneumonitis can be occurred in local intensity roughness and variation can cause increasing the density on the CT image, which is important factors in predicting RP. Moreover, the shape features were extracted from dosimetric-based segmentation, which reflect dose-volume histogram metrics. Thus, dosimetric parameters are essential for the prediction of the RP grade. For radiomics features in the dosimetric-based segmentation, the regions of the normal lung that received 60 Gy were selected as an important predictor in addition to the region of the normal lung that received 20 and 30 Gy. Although there are many reports that emphasize the importance of the median [27], the correlation between a high dose and RP has not been fully analyzed. We previously reported the importance of reducing high doses by analyzing NSCLC patients who received 3D-CRT or intensity-modulated RT (IMRT) [12]. The current study supports the importance of the higher dose as well as the median dose. We should reduce not only low and middle doses but also higher doses to prevent RP.

The problem with the previous radiomics analysis is that it is calculated from one value in the segmented region. RP mostly occurs in the locally irradiated lung. Multi-region analysis can extract radiomics features from the locally irradiated region in addition to the whole lung. Hao et al. proposed a predictive model for distant failure by shell analysis. Shell analysis extracts features in the boundaries of the tumor, which allows us to detect its associations with metastases within the microenvironment [28]. The current study also demonstrated that the radiomics features extracted in the multi-locally segmented region could be an important predictor of the classification of above and under RP grade 2 .

For feature selection with LASSO regression, all radiomics features extracted by texture analysis were used with the wavelet filter. Nie et al. reported that radiomics features with high-order filters and wavelets were significant predictors for differentiating focal nodular hyperplasia from hepatocellular carcinoma in the liver [28]. In the current study, all radiomics features with wavelet filters that were selected using LASSO regression were important predictors for the prediction of the RP grade. The imaging filter can denoise, smoothen, or enhance edges, and extract or eliminate a constant frequency. This leads to elimination of redundant and effective factors for prediction.

There were some limitations to the current study. Dosiomics and clinical factors such as smoking history, age, and chemotherapy could be integrated into the model to improve its prediction ability and robustness. Liang et al. proposed a prediction model for RP grade using dosiomics analysis from dose distribution for radiotherapy response prediction [29]. Although the multi-region radiomics analysis has improved the prediction ability compared to dosiomics analysis, dosiomics analysis can extract spatial features such as local intensity variation of the dose distribution and the ratio of the low-dose region. Future studies will be performed with a combination model of multi-region radiomics and dosiomics. Another limitation was that the current study used a dataset from a single institution of patients who underwent 3D-CRT. In the future, we will conduct a larger multicenter study using both 3D-CRT and IMRT data to construct a highly versatile predictive model. Ambiguity in the definition of grade 2 pneumonitis

may be another limitation as in the past report. In previous reports, the incidence of grade 2 pneumonitis varied considerably, and one of the causes may be that the definition was different in each paper. In this study, the definition of grade 2 RP was based on CTCAE ver.5.0. We tried to minimize subjective judgment by defining it as RP that need some kind of treatment. Still, we successfully combined both individual patient background factors and dosimetric factors by analyzing RP with our new Radiomics methods. Based on the prediction method developed in this study, it may be possible to reexamine the treatment plan by analyzing the images of the treatment plan and predicting the risk of Grade 2 pneumonitis before the start of treatment.

5. Conclusion

The developed multi-region radiomics analysis can help predict grade 2 RP for NSCLC after definitive radiotherapy. The radiomics features in the median and high-dose regions, and that of local intensity roughness and variation were important factors in predicting grade 2 RP.

Declarations

Conflict of Interest Statements

None

Funding: None

Contribution: Daisuke Kawahara and Nobuki Imano,wrote the main manuscript text and Riku Nishioka, Kouta Ogawa prepared the figures 1 and 2. Tomoki Kimura, Taku Nakashima, Hiroshi Iwamoto, Kazunori Fujitaka, Noboru Hattori, and Yasushi Nagata commented the manuscript and the research plan.

Acknowledgements

We gratefully acknowledge the Mathworks, Inc. for providing technical support.

References

1. Charles, B. & Simone Thoracic Radiation Normal Tissue Injury. *Semin Radiat Oncol.* **27** (4), 370–377 (2017).
2. Antonia, S. J. *et al.* Overall survival with durvalumab after chemoradiotherapy in stage iii nsclc. *N Engl J Med.* **379**, 2342–2350 (2018).
3. Yom, S. S. *et al.* Initial evaluation of treatment-related pneumonitis in advanced-stage non-small-cell lung cancer patients treated with concurrent chemotherapy and intensity-modulated radiotherapy. *Int J Radiat Oncol Biol Phys.* **68** (1), 94–102 (2007).
4. Sura, S. *et al.* Intensity-modulated radiation therapy (IMRT) for inoperable non-small cell lung cancer: The Memorial Sloan-Kettering Cancer Center (MSKCC) experience. *Radiotherapy and Oncology.* **87**,

17–23 (2008).

5. Allen, A. M. *et al.* Fatal pneumonitis associated with intensity-modulated radiation therapy for mesothelioma. *Int J Radiat Oncol Biol Phys.* **65**, 640–645 (2006).
6. Rice, D. C. *et al.* Dose-Dependent Pulmonary Toxicity After Postoperative Intensity-Modulated Radiotherapy for Malignant Pleural Mesothelioma. *Int J Radiat Oncol Biol Phys.* **69**, 350–357 (2007).
7. Jin, H. K. L. H. *et al.* Dose-volume thresholds for the risk of treatment-related pneumonitis in inoperable non-small cell lung cancer treated with definitive radiotherapy. *Radiother Oncol.* **91** (3), 427–432 (2009 Jun).
8. Marks, L. B. *et al.* Radiation dose-volume effects in the lung. *Int J Radiat Oncol Biol Phys.* **76** (3 Suppl), S70–S76 (2010).
9. Tucker, S. L. *et al.* Analysis of radiation pneumonitis risk using a generalized Lyman model. *Int J Radiat Oncol Biol Phys.* **72**, 568–574 (2008).
10. Marks, L. B. *et al.* Radiation dose-volume effects in the lung. *Int J Radiat Oncol Biol Phys.* **76** (3 Suppl), S70–S76 (2010).
11. Tucker, S. L. *et al.* Analysis of radiation pneumonitis risk using a generalized Lyman model. *Int J Radiat Oncol Biol Phys.* **72**, 568–574 (2008).
12. XXXX.
13. Lambin, P. *et al.* Radiomics: extracting more information from medical images using advanced feature analysis. *European journal of cancer.* **48**, 441–446 (2012).
14. Gierada, D. S. *et al.* Patient selection for lung volume reduction surgery - An objective model based on prior clinical decisions and quantitative CT analysis. *Chest.* **117**, 991–998 (2000).
15. Krafft, S. P., Rao, A. & Stingo, F. The utility of quantitative CT radiomics features for improved prediction of radiation pneumonitis. *Med Phys.* **45** (11), 5317–5324 (2018).
16. Hao, H., Zhou, Z., Li, S. & Maquilan, G. Shell feature: a new radiomics descriptor for predicting distant failure after radiotherapy in non-small cell lung cancer and cervix cancer. *Phys Med Biol.* **3** (9), 095007 (2018).
17. Xie, C. *et al.* Sub-region based radiomics analysis for survival prediction in oesophageal tumours treated by definitive concurrent chemoradiotherapy. *EBioMedicine.* **44**, 289–297 (2019).
18. National Cancer Institute. Common Terminology Criteria for Adverse Events (CTCAE) Version 5.0. Available online: http://ctep.cancer.gov/protocolDevelopment/electronic_applications/ctc.htm (accessed on 27 November 2017).
19. Yao, B., Wang, Y. D. & Liu, Q. Z. Radiation pneumonitis in non-small-cell lung cancer patients treated with helical tomotherapy. *Niger J Clin Pract.* **19**, 25–29 (2016).
20. Shi, S. *et al.* Risk factors associated with symptomatic radiation pneumonitis after stereotactic body radiation therapy for stage I non-small cell lung cancer. *Technol Cancer Res Treat.* **16**, 316–320 (2017).

21. Jjm, V. G. *et al.* Computational Radiomics system to decode the radiographic phenotype. *Cancer Res.* **77**, e104 (2017).
22. Tibshirani, R. Regression shrinkage and selection via the lasso: a retrospective. *J R Stat Soc Series B Stat Methodol.* **73**, 273–282 (2011).
23. Zhang, J. X. *et al.* Prognostic and predictive value of a microRNA signature in stage II colon cancer: a microRNA expression analysis. *Lancet Oncol.* **14** (13), 1295–1306 (2013).
24. Jun, D. *et al.* Predictors of grade ≥ 2 and grade ≥ 3 radiation pneumonitis in patients with locally advanced non-small cell lung cancer treated with three-dimensional conformal radiotherapy. *Acta Oncol.* **52** (6), 1175–1180 (2013).
25. Antonia, S. J. *et al.* Overall survival with durvalumab after chemoradiotherapy in stage iii nsclc. *N Engl J Med.* **379**, 2342–2350 (2018).
26. Jenkins, P. & Welsh, A. Computed tomography appearance of early radiation injury to the lung: correlation with clinical and dosimetric factors. *Int J Radiat Oncol Biol Phys.* **81(1)** (1), 97–103 (2011 Sep).
27. Marks, L. B. *et al.* Radiation dose-volume effects in the lung. *Int J Radiat Oncol Biol Phys.* **76** (3 Suppl), S70–S76 (2010).
28. Nie, P. *et al.* A CT-based radiomics nomogram for differentiation of focal nodular hyperplasia from hepatocellular carcinoma in the non-cirrhotic liver. *Cancer Imaging.* **20**, 20 (2020).
29. Liang, B. *et al.* Extracting 3D Spatial Features From Dose Distribution to Predict Incidence of Radiation Pneumonitis. Front. Oncol 2019; 12;9:269.

Figures

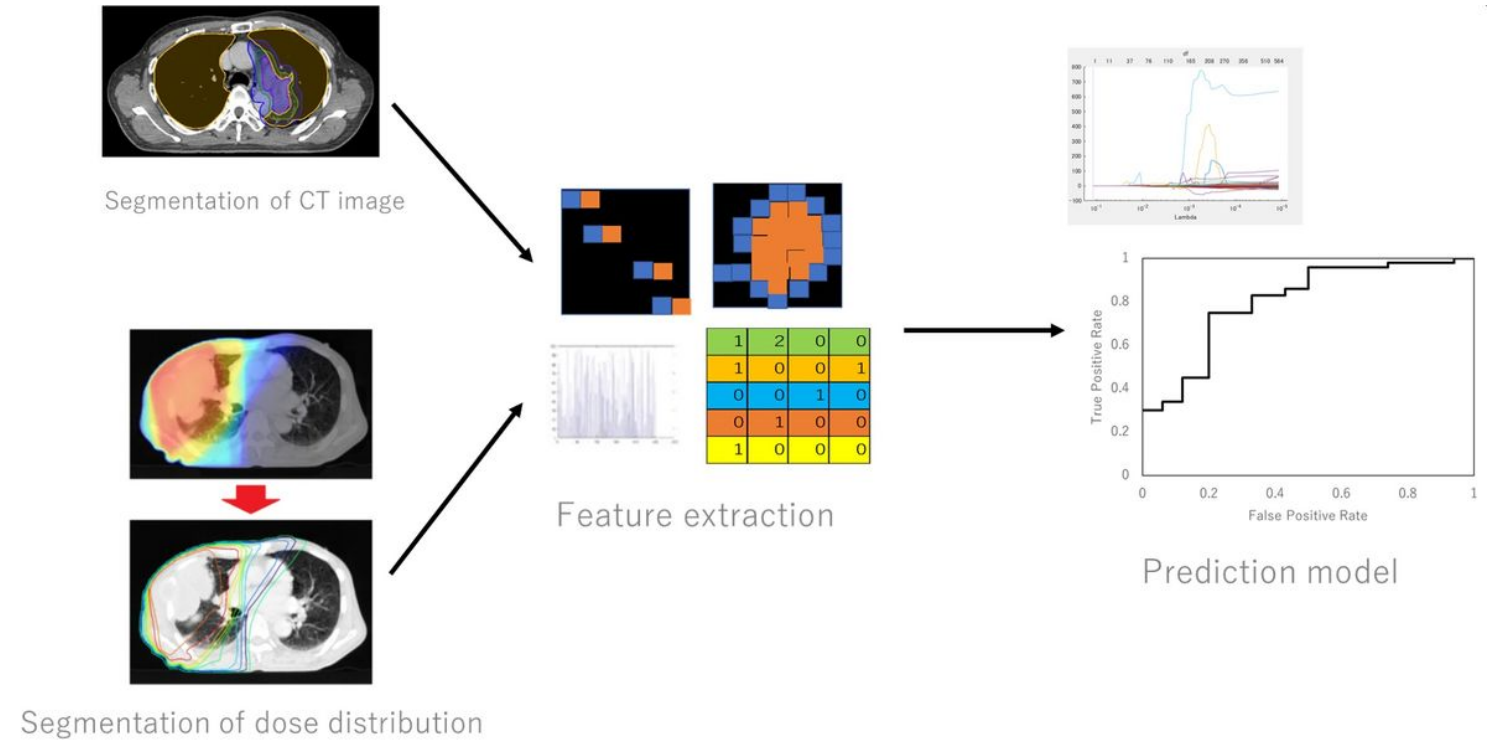

Figure 1

The process of the radiomics analysis and create prediction model.

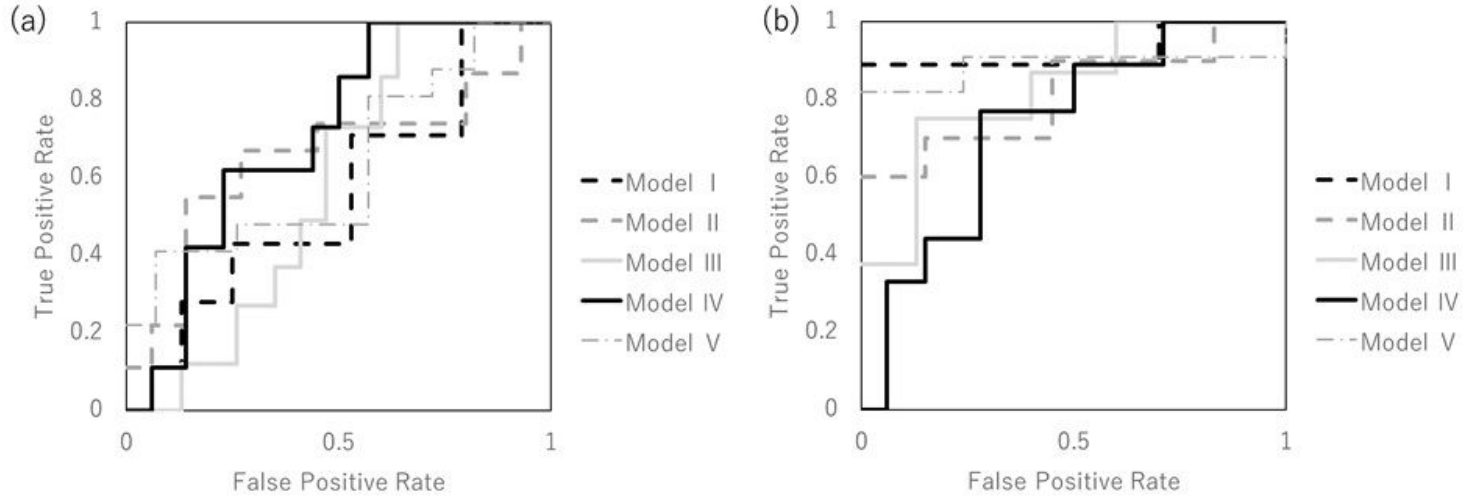

Figure 2

The performance of the predictive model was validated according to the ROC metrics with 5-fold cross validation in the whole-lung-region radiomics (a) and multi-region radiomics analysis (b).

Supplementary Files

This is a list of supplementary files associated with this preprint. Click to download.

- SupplementalTable.docx
- SF1.tif
- SF2m.tif
- SF3m.tif